

AD-A285 158



January 1994

Final, 24-27 January 1994

Temperature dependence of laser induced breakdown

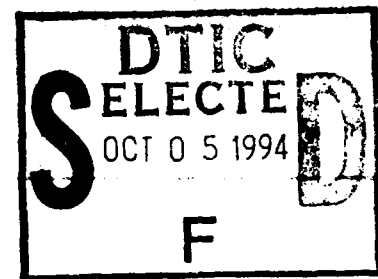
PR - 2312
TA - A1
WU - 01



Daniel X. Hammer Stephen A. Boppart
Rex Eiserer Paul Kennedy
Gary D. Noojin W.P. Roach

Armstrong Laboratory (AFMC)
Occupational and Environmental Health Directorate
Optical Radiation Division
Brooks AFB, TX 78235

AL/OE-PC-1994-0004



Approved for public release; distribution is unlimited.

The physical properties of laser-induced optical breakdown (LIB) in highly transparent, dispersive media, like that found in the eye, are of great interest to the ophthalmic community. We examined the temperature dependent characteristics of LIB thresholds in media with a temperature range of 20°C to 80°C using nanosecond, picosecond, and femtosecond pulses produced in the visible and near infrared spectral regions. Media used for these studies included high purity water, tap water, physiological (0.9%) saline solution, and bovine vitreous. 10ns pulses at 532 nm and 60 ps and 90 fs pulses at 580 nm were focused into a sample to produce LIB. Probit analysis was used to determine the 50% probability threshold value (ED_{50}) as the temperature of the media was varied. Additional data was obtained by keeping pulse energy constant and varying temperature. ED_{50} values for LIB showed no consistent dependence on the temperature of the medium. The theory of the temperature dependence of LIB and experimental observations for all pulse durations and their implications for retinal damage are discussed.

Laser Induced Breakdown, temperature dependence, threshold value,
nanosecond, picosecond, femtosecond, laser pulses

11

Unclassified

Unclassified

Unclassified

UL

GENERAL INSTRUCTIONS FOR COMPLETING SF 298

The Report Documentation Page (RDP) is used in announcing and cataloging reports. It is important that this information be consistent with the rest of the report, particularly the cover and title page. Instructions for filling in each block of the form follow. It is important to **stay within the lines to meet optical scanning requirements.**

Block 1. Agency Use Only (Leave Blank)

Block 2. Report Date. Full publication date including day, month, and year, if available (e.g. 1 Jan 88). Must cite at least the year.

Block 3. Type of Report and Dates Covered. State whether report is interim, final, etc. If applicable, enter inclusive report dates (e.g. 10 Jun 87 - 30 Jun 88).

Block 4. Title and Subtitle. A title is taken from the part of the report that provides the most meaningful and complete information. When a report is prepared in more than one volume, repeat the primary title, add volume number, and include subtitle for the specific volume. On classified documents enter the title classification in parentheses.

Block 5. Funding Numbers. To include contract and grant numbers; may include program element number(s), project number(s), task number(s), and work unit number(s). Use the following labels:

C - Contract	PR - Project
G - Grant	TA - Task
PE - Program Element	WU - Work Unit Accession No.

Block 6. Author(s). Name(s) of person(s) responsible for writing the report, performing the research, or credited with the content of the report. If editor or compiler, this should follow the name(s).

Block 7. Performing Organization Name(s) and Address(es). Self-explanatory.

Block 8. Performing Organization Report Number. Enter the unique alphanumeric report number(s) assigned by the organization performing the report.

Block 9. Sponsoring/Monitoring Agency Name(s) and Address(es). Self-explanatory.

Block 10. Sponsoring/Monitoring Agency Report Number. (If known)

Block 11. Supplementary Notes. Enter information not included elsewhere such as: Prepared in cooperation with...; Trans. of ..., To be published in When a report is revised, include a statement whether the new report supersedes or supplements the older report.

Block 12a. Distribution/Availability Statement. Denote public availability or limitation. Cite any availability to the public. Enter additional limitations or special markings in all capitals (e.g. NOFORN, REL, ITAR)

DOD - See DoDD 5230.24, "Distribution Statements on Technical Documents."
DOE - See authorities
NASA - See Handbook NHB 2200.2.
NTIS - Leave blank.

Block 12b. Distribution Code.

DOD - DOD - Leave blank
DOE - DOE - Enter DOE distribution categories from the Standard Distribution for Unclassified Scientific and Technical Reports
NASA - NASA - Leave blank
NTIS - NTIS - Leave blank.

Block 13. Abstract. Include a brief (Maximum 200 words) factual summary of the most significant information contained in the report.

Block 14. Subject Terms. Keywords or phrases identifying major subjects in the report.

Block 15. Number of Pages. Enter the total number of pages.

Block 16. Price Code. Enter appropriate price code (NTIS only).

Blocks 17. - 19. Security Classifications. Self-explanatory. Enter U.S. Security Classification in accordance with U.S. Security Regulations (i.e., UNCLASSIFIED). If form contains classified information, stamp classification on the top and bottom of the page.

Block 20. Limitation of Abstract. This block must be completed to assign a limitation to the abstract. Enter either UL (unlimited) or SAR (same as report). An entry in this block is necessary if the abstract is to be limited. If blank, the abstract is assumed to be unlimited.

PROCEEDINGS REPRINT

 SPIE—The International Society for Optical Engineering

Reprinted from

Proceedings of

Laser-Tissue Interaction V

**24-27 January 1994
Los Angeles, California**

Accession for	
NTIS CRA&I	<input checked="" type="checkbox"/>
DTIC TAB	<input type="checkbox"/>
Unannounced	<input type="checkbox"/>
Justification	
By	
Distribution/	
Availability Codes	
Dist	Avail and/or Special
A-1	20



Volume 2134A

©1994 by the Society of Photo-Optical Instrumentation Engineers
Box 10, Bellingham, Washington 98227 USA. Telephone 206/676-3290.

94-31585



94 10 1 21

Temperature dependence of laser induced breakdown

Daniel X. Hammer¹, Rex Eiserer¹, Gary D. Noojin²,
Stephen A. Boppart³, Paul Kennedy¹, and W. P. Roach¹

¹Optical Radiation Division, Armstrong Laboratory, Brooks AFB, Texas 78235

²The Analytic Science Corporation, San Antonio, Texas 78235

³Massachusetts Institute of Technology, Department of Electrical Engineering,
Cambridge, Massachusetts 02139

ABSTRACT

The physical properties of laser-induced optical breakdown (LIB) in highly transparent, dispersive media, like that found in the eye, are of great interest to the ophthalmic community. We examined the temperature dependent characteristics of LIB thresholds in media with a temperature range of 20°C to 80°C using nanosecond, picosecond, and femtosecond pulses produced in the visible and near infrared spectral regions. Media used for these studies included high purity water, tap water, physiological (0.9%) saline solution, and bovine vitreous¹. 10 ns pulses at 532 nm and 60 ps and 90 fs pulses at 580 nm were focused into a sample to produce LIB. Probit analysis was used to determine the 50% probability threshold value (ED_{50}) as the temperature of the media was varied. Additional data was obtained by keeping pulse energy constant and varying temperature. ED_{50} values for LIB showed no consistent dependence on the temperature of the medium. The theory of the temperature dependence of LIB and the experimental observations for all pulse durations and their implications for retinal damage are discussed.

2. INTRODUCTION

The practical application of laser induced breakdown (LIB) has been studied extensively in the medical community². The characterization of the propagation of ultrashort (subnanosecond) laser pulses through various media and the interaction of the pulse with the media is of fundamental importance in these studies. To the medical community, the generation and control of the plasmas produced by LIB has direct application to ophthalmic surgery as a tool for ocular tissue disruption. Currently, LIB is used in ophthalmic surgery in three different techniques: to remove the opaque posterior capsule (capsulotomy) in cataract surgery after the intraocular lens has been implanted³; to remove pressure in the eye by piercing the iris in patients with glaucoma⁴; and to remove vitreal strands that form in the anterior of the vitreous⁵. LIB and its associated bubble formation and acoustic shock wave generation may also cause hemorrhagic lesions when laser light is focused on the retina⁶. The characterization of LIB, in particular an accurate measure of the threshold, remains a top priority in order to study the true interaction of laser radiation with the eye.

LIB occurs when laser irradiance reaches a threshold for a particular medium. This threshold depends on numerous pulse characteristics, such as duration, wavelength, focal spot size, spatial/temporal profile, and medium characteristics such as impurity concentration⁷. Thresholds have been determined in the past for various focal spot sizes⁸, and different focal length lenses⁹, but often lack detailed supporting information about the pulse spatial/temporal profile and the medium's physical characteristics. Our goal, therefore, was to quantitatively measure one medium characteristic that has heretofore been ignored.

When a sufficient amount of thermal energy ($k_B T$, k_B = Boltzmann's constant) is introduced into the sample not only will the population of translational, rotational, and vibrational excited states increase, but the population of higher electronic states as well. We applied this idea to LIB phenomena observed in physiological solutions like tap water, saline, and bovine vitreous. We assume that as the temperature

increased, the population of electrons residing in excited states would increase. With an increase of excited electrons within the Rayleigh range of the focused pulse, statistically the number of sufficiently energetic electrons available to interact with the pulse (photons) and initiate a breakdown event will increase with the rise in temperature. Providing our assumptions held true, we hypothesize a lowering of the threshold energy (or irradiance) required to induce breakdown with increased sample temperature.

We believe that if an accurate measure of a temperature dependence could be made in the range of 20°C to 80°C, then a model could be developed to determine the activation energy required for LIB initiation and potentially determine the species most likely to contribute the initiating electrons. Further, and more importantly to the study of ocular damage from subnanosecond laser pulses, most threshold studies of LIB associated with safety or medical research report data obtained at 21 - 25 °C instead of 35 - 37 °C. We seek to determine if the difference in temperature makes any significant contribution to the amount of energy per subnanosecond pulse required to initiate LIB in vivo.

3. LASER INDUCED BREAKDOWN

LIB is an all-or-none process, yet it is highly statistical and probabilistic and hence, threshold measurements tend to be inexact. Thresholds typically are represented as an energy or an irradiance at which there is a 50% or 100% probability that LIB will occur. Thresholds also have a large standard deviation. LIB occurs by either avalanche or multiphoton ionization. Avalanche ionization occurs when a seed electron absorbs photons, accelerates, and frees bound electrons by collisional ionization. These electrons in turn accelerate and free more electrons, and the process cascades into a volume of plasma. Avalanche ionization is likely to occur in the nanosecond time regime where the pulse is relatively long compared to the collisional ionization time. This mechanism is highly impurity dependent. Multiphoton ionization occurs when each bound electron is ionized by absorption of multiple photons. Each electron acts independently and no electron-to-electron interactions are required. Multiphoton ionization is likely to occur in the femtosecond time regime and a transition between the two processes occurs in the picosecond regime. With multiphoton ionization, electrons are stripped and ions are created simultaneously with very little impurity concentration dependence^{10,11}.

4. EXPERIMENTAL SETUP

4.1. Laser System Setup

The ultrashort laser system setup for producing nanosecond to femtosecond pulses is shown in Figure 1. The system is made from off-the-shelf components built by Spectra-Physics. The primary pulse comes from a Model 3800 Mode-locked Nd:YAG laser which generates 80 ps pulses at 82 MHz pulse repetition frequency (PRF), 1064 nm, and approximately 11.5 W. The pulses are compressed to 5 ps with a fiber/grating compressor and frequency doubled to 532 nm in the Model 3695 Optical Pulse Compressor. The power output from the 3695 is approximately 1 W. The pulse is then sent through the Model 3500 rhodamine dye laser which is synchronously pumped by the 3800. The output from the 3500 is from 3 ps to 300 fs at 570 nm and 150 mW. This pulse duration is verified with a Model 409 fast scan autocorrelator. The pulses from the 3500 are chirped in a second fiber in the CPA-2 Chirper. The output from the chirper is in the nJ range at 570 nm with a 30 nm bandwidth. The chirped pulse is then delayed and amplified approximately 0.5 million times to 100 μ J in a PDA-1 three stage Kiton red dye amplifier. The dye amplifier is pumped by the GCR-3RA Nd:YAG Regenerative Amplifier that operates at either 5 ns or 80 ps, 532 nm, 50 mJ, and an adjustable pulse repetition frequency of single pulse mode to 10 Hz. The GCR is seeded by the 3800 to maintain timing of the pulses. The optical delay is included to allow both the pulse from the GCR and the chirped pulse from the 3800 to enter the dye amplifier at the same time. The output pulse is then rephased in the CPA-2 Prism Rephaser Module. The optimum output of the laser system is a 570 nm, 90 fs, 100 μ J pulse that operates in single shot to 10 Hz mode. The pulse duration of the picosecond and femtosecond pulses are measured at the output with an Inrad Slow Scan

Autocorrelator. The pulse profile is approximately 80% Gaussian and is monitored with a Cohu CCD camera input to the Photon BeamGrabber beam profiler continuously during the experiment.

The most useful feature of the laser system is the wide variety of wavelengths, pulse durations and energy levels available with relative ease of reconfiguration. This is done by picking the pulse off at different points in its progression through the system. For example, 300 fs pulses may be created by bypassing the CPA-2 pulse compressor. In addition, the laser system is modular, and only the shortest pulses require all of the units to operate simultaneously. All output pulses have energies greater than 100 μ J, and at some wavelengths pulses are of the order of millijoules. The output wavelength is determined by the pulse dye amplifier bandwidth, and the chirped pulse from the dye laser must match this bandwidth in order to be completely amplified. Otherwise, when the amplified pulses are recombined, the pulsewidth will not be 90 fs or shorter. Pulses at a wavelength of 580 nm are obtained for pulsewidths of 90, 300, and 800 fs, and 1 to 3 ps. Pulses at a wavelength of 532 nm are obtained for pulsewidths of 50 ps with the seeded Nd:YAG regenerative amplifier and 5 ns with the unamplified Nd:YAG Q-switched laser, with pulse energies for both in the millijoule range. If average power is needed rather than energy, modelocked output pulses at 82 MHz are obtained at 532 nm and 800 mW, and at 570-640 nm at 200 mW without amplification.¹²

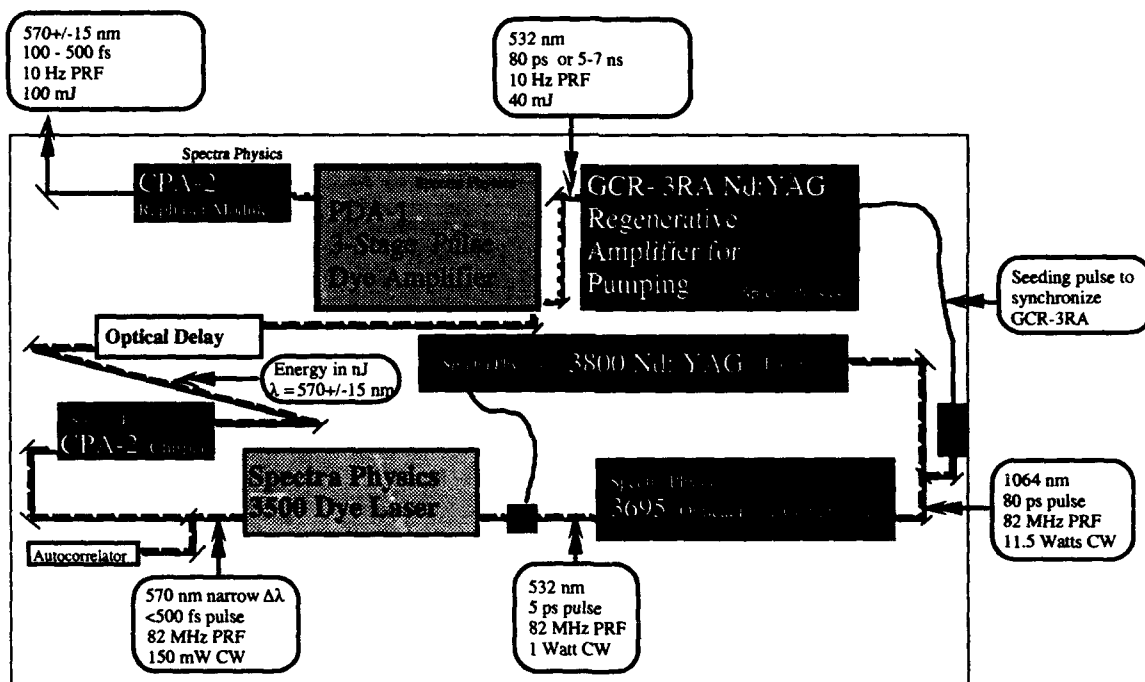


Figure 1: Schematic of Ultrashort Pulse Laser System used for LIB threshold measurements at Brooks AFB.

The nanosecond pulses were produced with a Spectra-Physics DCR-11 Nd:YAG Laser that operates at 1064 nm, 10 ns, 50 mJ, and from single shot to 10 Hz mode. The pulse duration is verified with a Scientech PIN diode, whose response curve is read off a Tektronix 602A digitizing oscilloscope continuously during the experiment. The pulse profile is approximately 80% Gaussian as verified with a Cohu CCD camera input to Beamcode beam analysis software by Big Sky Software Corporation.

4.2. Optical Setup

The optical setup is shown in Figure 2. The pulse energy from either the Ultrashort Pulse Laser System or the Spectra-Physics DCR-11 is measured at A1 to verify the energy entering the optical setup and the percentage of light split by the first beamsplitter, BS1. The amount of energy split by a beamsplitter varies slightly with polarization and wavelength of the pulse. The detectors were either J50, J25, or J4 Molecron detectors output to a Molecron JD2000 Joulemeter Ratiometer. M2 is placed in the setup to measure the energy ratio $B1/A2$. During the experiment the pulse proceeds through L1, a 17 mm aspheric lens which focuses the pulse down to a spot size diameter of approximately $25 \mu\text{m}$ in a cuvette of water. The 17 mm aspheric models the 17.1 reduced focus of the eye¹³. The spot size was verified with a knife edge measurement in both air and a cuvette of water. The cuvette is an L-shaped jacketed cell that has two chambers, one for the media and one connected by Tygon tubing to the pump of the MGW Lauda RC-6 temperature controlling bath. The output pulse from the cuvette is recollimated by either another 17 mm aspheric lens or a 25 mm spherical lens with wider aperture than the 17 mm lens. The energy is measured out of the cell, A3, at the beginning of each run to measure the ratio of energy split by BS2. The output energy is recorded at A4. The other arm of the split pulse is sent into the Cohu camera for beam profiling. The neutral density filters (ND) block the light to a level that prevents the camera from saturating. The plasma is imaged with two lenses of focal length 230 mm and 140 mm onto the Hitachi CCTV camera. The filter F1 is one of two beamsplitters which splits either 580 nm or 532 nm at 45° and passes all other wavelengths. The image is monitored on a black and white TV which is viewed to determine if a plasma has formed.

The determination of whether LIB occurred, for all pulse durations, was visual. In the nanosecond time regime, the visible flash from the infrared laser pulse, as well as the loud snapping sound from the resultant supersonic shock wave made LIB discernment obvious. In the pico- and femtosecond time regimes, the image viewed on video of light passing through the filter F1, was sufficient to determine the existence of the LIB event. The gain was high enough to saturate the camera when LIB occurred. However, in the pico- and femtosecond regimes, there was no auditory signal accompanying the LIB to aid in distinguishment. In addition, the small size of the plasma in the femtosecond regime made determination particularly difficult.

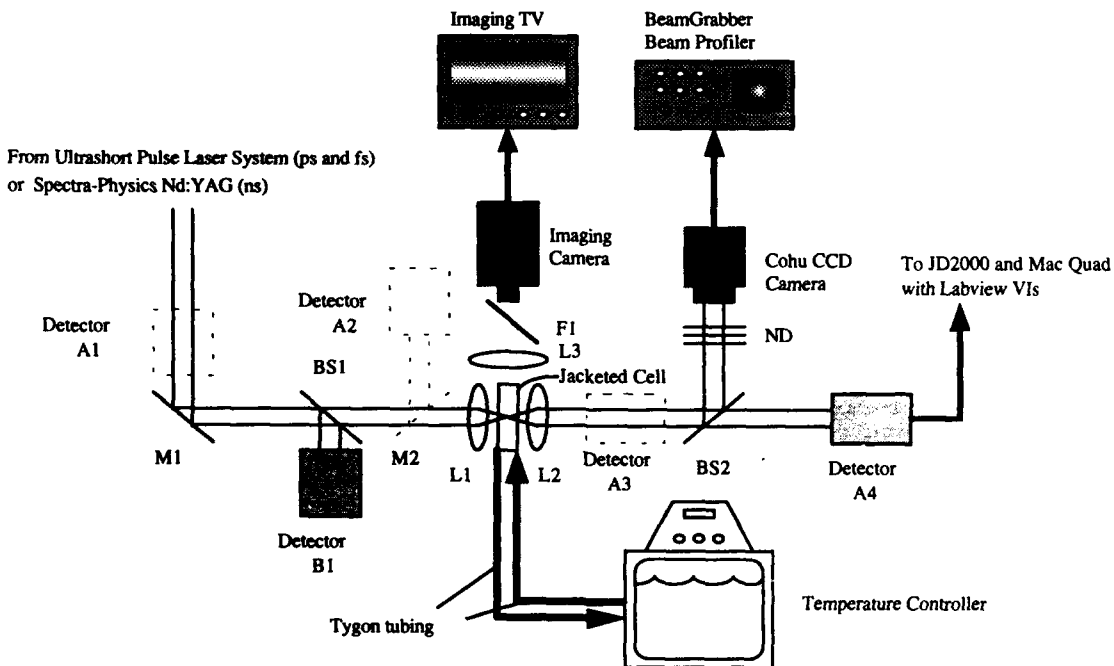


Figure 2: Optical setup used for temperature dependence studies.

4.3. Energy Measurement

The energy is measured and recorded at a number of points in the setup at the beginning of each run to determine the losses from particular optical elements. The energy from the Ultrashort Pulse Laser System or the Spectra-Physics Nd:YAG laser into the setup is measured at A1. The energy ratios A3/B1 and A4/B1 are measured to verify the losses from the lenses and second beamsplitter BS2. The ratio of energy that enters into the lens/cell configuration is measured by A2/B1.

During each temperature run, the energies at A4 and B1 are measured by the JD2000 and sent to the National Instruments Labview software virtual instrument (VI). The ratio A2/B1 is multiplied by the measured energy from B1 to get the adjusted energy into the cell (E_{in}). A probability versus E_{in} curve was generated with this procedure.

4.4. Temperature Control

Temperature control is accomplished in the setup with a jacketed cuvette and temperature controlled bath. The temperature control for the bath is within $\pm 0.1^\circ\text{C}$. The temperature control of the media in the cuvette is within $\pm 0.25^\circ\text{C}$. The temperature of the media is measured with a Markson Model 95 Digital Temperature Meter and a Yellow Springs Instrument Model 700 probe. The range of temperatures measured is from 20°C to 80°C in increments of 10°C . To maintain physiological characteristics we chose not to measure sample temperatures near the freezing or boiling points.

4.5. Statistical Analysis

Due to the probabilistic nature of LIB, a method of calculating the thresholds for breakdown based upon a normal distribution of data points is needed. Probit analysis¹⁴ is one means of calculating the probability of breakdown versus energy dose delivered to a cuvette of media. Probit curves and fiducial limits were computed on Statistical Analysis System (SAS). Probit curves give the probability that an energy dose will cause breakdown. The probability is usually reported as an ED_{xx} value which gives the $xx\%$ probability that a certain event will occur. In addition, probit analysis gives fiducial limits of the probability which express the confidence limits of a probability. Figure 3 gives a typical probit curve with 95% fiducial limits. For example, Figure 3 shows an ED_{50} of 0.275 mJ with upper and lower fiducial limits of 0.312 mJ and 0.243 mJ for tap water at 50°C and laser pulse duration of 60 ps. The negative energy values are an artifact of Probit Analysis.

The error bars of the ED_{50} versus temperature curve are calculated by taking the root-sum-square of the 95% fiducial limits and the instrument uncertainty of the adjusted input energy. The error bars presented in Figures 4 and 5 may not fully represent the uncertainty of the data for this size data set. For example, the error bars should include any fluctuations in the laser system but do not include fluctuations in spot size, which are impossible to measure during the experiment. Therefore, the actual uncertainties may be somewhat larger than the ones presented in Figures 4 and 5.

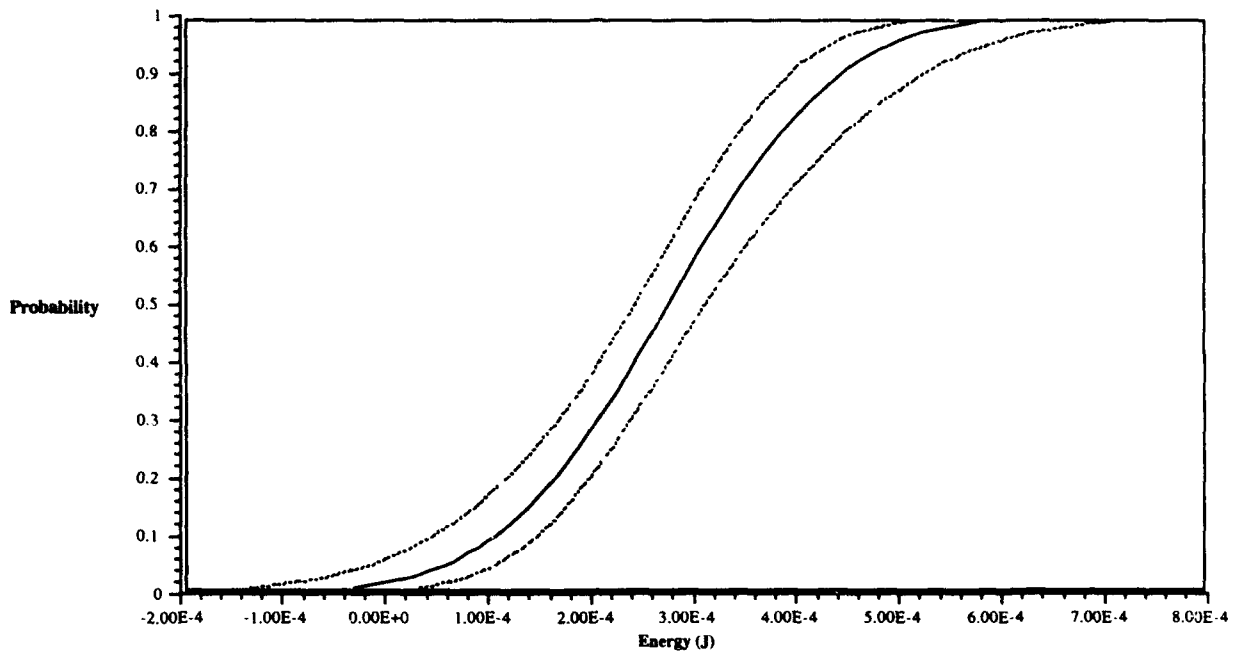


Figure 3: Shown is a typical probit curve (solid line) and 95% fiducial limits (dotted lines) for tap water at 50°C and laser pulse duration of 60 ps.

5. RESULTS

5.1 First Method

The first method used to attempt to resolve a temperature dependence was described above. The temperature was held constant and the energy was varied from the energy at which there is 0% probability of breakdown to the energy at which there is 99% probability of breakdown. The order of the temperature data was random, insuring no time dependence or other unmeasurable effect of the laser system that may skew the data over the course of the experiment. Approximately 200 single shot pulses were delivered to the cuvette to produce a probit curve.

5.1.1 Nanosecond Time Regime

Figure 4 shows the nanosecond ED_{50} breakdown threshold versus temperature. The difference in threshold levels for different media is noted and has been studied previously^{15,16,17}. The average threshold for bovine vitreous decreased constantly from 3.85 mJ at 20°C to 2.87 mJ at 80°C. However, all the values fall within the error bars. The threshold for saline, high purity water, and tap water exhibited large variation but no clear trend. The large discontinuity in threshold for high purity water from 30°C to 40°C suggests a statistically significant downward temperature trend. The slightly smaller drop from 40°C to 50°C and the increase from 50°C to 60°C for tap water also suggest a statistically significant change due to temperature. However, these observations are inconsistent with the vitreous and saline data.

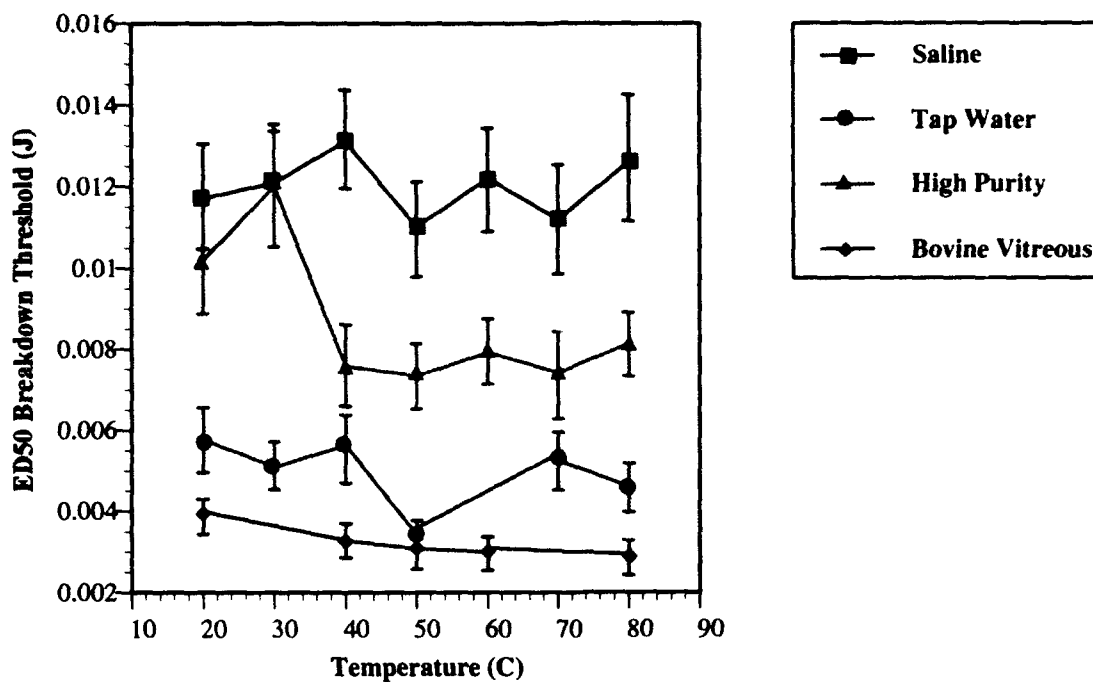


Figure 4: Graph represents the ED₅₀ LIB thresholds vs. temperature for 10 ns laser pulses. The Error Bars are the root-sum-square of 95% fiducial limits and uncertainty of energy measurement.

5.1.2 Picosecond Time Regime

Figure 5 shows the picosecond ED₅₀ breakdown threshold versus temperature. The results are similar to those found for the nanosecond time regime. For saline, all data points fell within the uncertainty. Tap 1 and tap 2 are runs from two successive days and exhibit the large variation found in this study. The difference between threshold levels for equivalent samples may be due to different impurity species that reside in each sample. With the exception of the data point at 80°C, all threshold values for tap 1 fell within the uncertainty. For tap 2, all data points except 30°C and 70°C fell within the uncertainty. As in the nanosecond data, these observations are inconsistent and further study is needed to explain this anomalous behavior.

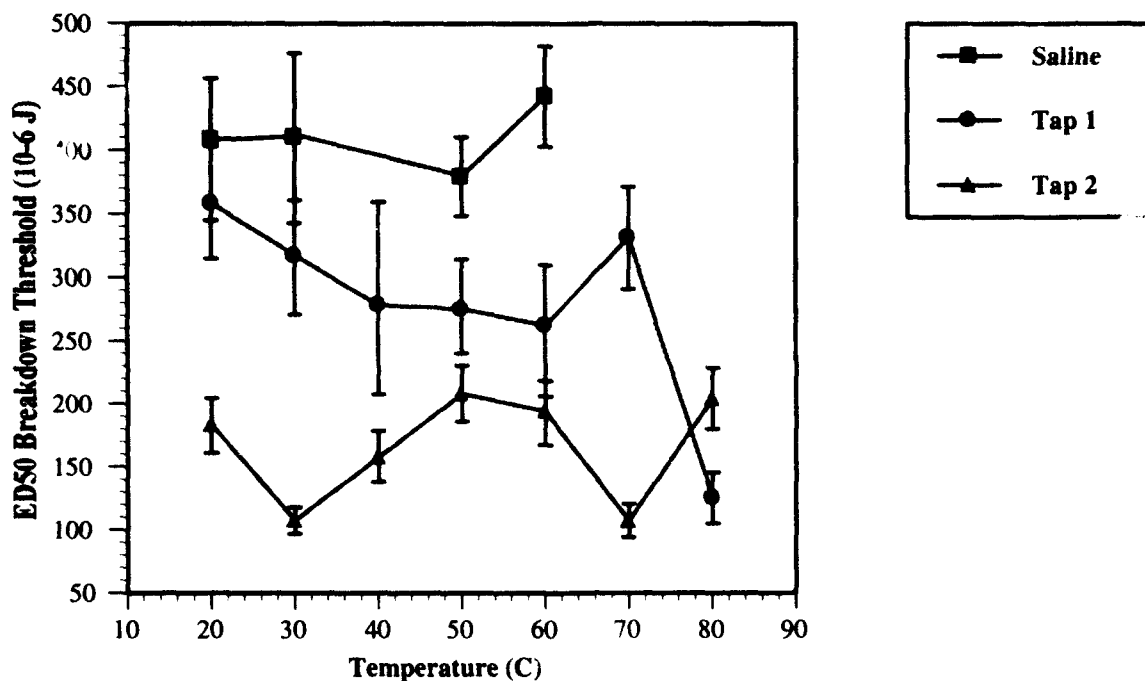


Figure 4: Graph represents the ED₅₀ LIB thresholds vs. temperature for 60 ps laser pulses. The Error Bars are the root-sum-square of 95% fiducial limits and uncertainty of energy measurement.

5.1.3 Femtosecond Time Regime

The femtosecond time regime yielded the least quantitative results but the most interesting observations of the nature of laser induced breakdown. Previous studies have found the ED₅₀ threshold of LIB to be approximately 1.5 μJ at 580 nm and 90 fs⁷. Our study observed the threshold for LIB at 90 fs to be much greater than 1.5 μJ. A more quantitative threshold for LIB at this pulse duration could not be found because the maximum energy the laser can output is approximately 100 μJ. The maximum energy the laser can delivered to the cuvette is approximately 50 μJ accounting for the optics in the system and setup. Therefore, a full probit curve could not be produced due to the limited energy output. Another observation exclusive to the femtosecond regime is the decreased recovery time of the media. With the pulses delivered single shot at a constant energy level, no LIB events were observed to occur. However, at the same constant energy, many LIB events were observed with the pulse repetition frequency of the laser at 10 Hz. This decreased recovery time was not due to electron recombination, acoustic, or thermal effects, which occur on the order of approximately 10⁻⁷, 10⁻⁶, and 10⁻⁵ seconds after the LIB event, respectively. Gas and bubble formation may explain the observed response of the media to femtosecond pulses at 10 Hz.

In addition, self-phase modulation (SPM) and bubble formation were observed to occur at approximately 1-2 μJ. This result is contrary to the results found in previous studies for longer pulse durations^{18,19} where the threshold for SPM is very close to the threshold for LIB. This lends further credence to the postulate of two distinct types of plasmas at this pulse duration each at a different irradiance threshold¹⁵. The hot plasma, occurring at the higher threshold, produces a visible broadband flash in all directions and is similar to the plasmas produced at other durations with the exception of the threshold level. The cold plasma, occurring at a much lower threshold, is without a broadband flash but with other characteristics associated with LIB, namely initiation by multiphoton ionization, continuum generation, and cavitation bubble formation. Continued study is needed to fully understand LIB at these

ultrashort pulse durations.

5.2 Second Method

The inconsistencies presented above in the first method led us to seek more precise experimental techniques to measure any temperature dependence. A second method was devised, in which the energy was held constant somewhere within the 0% and 99% probability of breakdown while the temperature was varied. Approximately 200 single shot pulses were delivered to the cuvette of media at a constant energy and temperature. The energy was windowed to a set energy range and for all cases had a standard deviation less than one tenth of the average energy delivered. Probit analysis was not used, with the expectation that by reducing as many areas of probability as possible, a more realistic threshold could be obtained and thus any slight variation in the temperature dependence measured.

Table I lists the percentage of negative responses obtained for three temperatures for tap water, high purity water, and saline at constant pulse energy. A decreasing percentage with increasing temperature would indicate a temperature dependence. Saline and tap water exposed to 60 ps pulses show the hypothesized decrease in percentage. The other sets of data all exhibit a large variation and no clear trend.

Table I: Percentage of Negative Responses for constant energy and varying temperature

	60 Picosecond			10 Nanosecond		
	High Purity	Saline	Tap Water	High Purity	Saline	Tap Water
24°C	50%	66.0	69%	79%	72%	62%
50°C	17%	48%	68%	63%	43%	71%
80°C	34%	39%	52%	72%	53%	58%

6. DISCUSSION

6.1 Experimental Discussion

The data presented above show no clear trend of temperature dependence. Some of the data may appear to exhibit a trend, such as the bovine vitreous in the first method and the saline in the second method. However, the large variability of all the thresholds discount any attempt to reach a positive conclusion based upon this data. This was due to the difficulty in consistently measuring the thresholds which are based on a probability curve without taking an inordinately large sample size. There were a multitude of effects that needed to be controlled to differentiate any supposed temperature dependence from the other factors.

6.2. Theoretical Discussion

Our measurements on ocular media using various pulsewidths showed no consistent temperature dependence large enough to resolve with current experimental techniques in the range from 20°C to 80°C. A first-order theoretical analysis, using optical absorption data for water, seems to support the conclusion that temperature dependence over this range will be small to negligible.

There are two ways increased temperature could, in theory, reduce the optical breakdown threshold of water and aqueous solutions. First, higher temperatures would increase the probability of molecular ionization through thermal collisions. If the increase in thermal ionization was significant over the temperature range considered, then the avalanche breakdown threshold would decrease due to increased initial (seed) electron density. This effect is unlikely due to the large ionization energy of water,

approximately $6.5 \text{ eV}^{20,21}$. At 80°C , $k_B T = 0.03 \text{ eV}$, a thermal energy far too low to give a statistically significant probability of ionization.

The second possibility is that higher temperatures could reduce the average ionization energy of the medium, which would reduce the threshold for both avalanche and multiphoton breakdown. UV absorption measurements in water, however, show that for temperature variation from 24°C to 80°C , transition energy decreases only 0.12 eV , roughly a 2% decrease²². Such a small decrease is unlikely to produce measurable changes in the breakdown threshold.

The comments above exclusively apply to ionization of water molecules. It is possible that impurities with very low binding energies may create a temperature dependent breakdown in aqueous solutions. Measurements in impure media such as tap water, however, have not shown this effect.

6.3. Conclusion

The conclusion of this study is that the LIB measured thresholds are not dependent on the temperature of the media in the range studied. Furthermore, the LIB threshold data measured at 21°C to 25°C presented in literature are valid *comparisons* to the LIB thresholds that occur at 35°C to 37°C in the eye.

In addition, valuable collateral information has been gained from this study. The observations of femtosecond pulses presented above in particular have led to discussion of the physical properties of the plasmas. The differences in the breakdown threshold and superbroadening threshold at this pulse duration could indicate an occurrence of nonlinear processes and need to be studied further. The decreased recovery time of the media in the femtosecond time regime is also puzzling considering most side effects of LIB have ceased by milliseconds after the event. In addition, the femtosecond breakdown thresholds need to be reevaluated to either validate or refute earlier threshold measurements.

7. ACKNOWLEDGMENTS

This work was supported by Armstrong Laboratory and AFOSR (2312A101). The authors would like to thank Reginald Birngruber, Alfred Vogel, Randy Thompson, Ben Rockwell, and Mark Rogers for their input into the theoretical discussions of temperature dependence of LIB.

8. REFERENCES

1. Animals involved in this study were procured, maintained, and used in accordance with the Animal Welfare Act and the "Guide for the Care and Use of Laboratory Animals" prepared by the Institute of Laboratory Animal Resources, National Research Council.
2. S. J. Gitomer and R. D. Jones, "Laser-Produced Plasmas in Medicine," *IEEE Transactions on Plasma Science*, Vol. 19, No. 6, p. 1209, 1991.
3. D. Aroa-Rosa, J. J. Aron, M. Greisemann, and R. Thyzel, "Use of the neodymium YAG laser to open the posterior capsule after lens implant surgery: a preliminary report," *Journal of the American Implants Society*, Vol. 6, p. 352, 1980.
4. A. L. Robin and I. P. Pollack, "The Q-switched ruby laser in glaucoma," *Ophthalmology*, Vol. 91, p. 366, 1984.
5. S. Lerman, B. Thrasher, and M. Moran, "Vitreous changes after Nd:YAG laser irradiation of the posterior lens capsule or mid-vitreous," *American Journal of Ophthalmology*, Vol. 97, p. 470, 1984.
6. J. A. Zuclich, W. R. Elliot, C. P. Cain, G. D. Noojin, W. P. Roach, B. A. Rockwell, C. A. Toth, "Ocular Damage Induced by Ultrashort Laser Pulses," *Armstrong Laboratory Technical Report*, AL/OE-TR-1993-0099, 1993.

7. S. A. Boppart, C. A. Toth, W. P. Roach, and B. A. Rockwell, "Shielding effectiveness of femtosecond laser-induced plasmas in ultrapure water," *SPIE Laser Tissue Interaction IV*, Vol. 1882, p. 347, 1993.
8. E. W. Van Stryland, M. J. Soileau, A. L. Smirl, and W. E. Williams, "Pulse-width and focal-volume dependence of laser-induced breakdown," *Physical Review B*, Vol. 23, No. 5, p. 2144, 1981.
9. W. L. Smith, J. H. Bechtel, and N. Bloembergen, "Dielectric-breakdown threshold and nonlinear-refractive-index measurements with picosecond laser pulses," *Physical Review B*, Vol. 12, No. 2, p. 2396, 1975.
10. C. A. Puliafito and R. F. Steinert, "Short Pulsed Nd:YAG Laser Microsurgery of the Eye. Biophysical Considerations," *IEEE Journal of Quantum Electronics*, Vol. QE-20, No. 12, p. 1442, 1984.
11. P. Kennedy, S. A. Boppart, "Optical Breakdown: A Conceptual Overview," Colloquium given at Brooks AFB on 8 March 1993.
12. C. P. Cain, "Ultrashort-Pulse Laser System: Theory of Operation and Operating Procedures," *Armstrong Laboratory Technical Report*, AL-TR-1991-0146, 1992.
13. M. Katz, Section Author, *Duane's Clinical Ophthalmology*, Vol. 1, Chapter 33, p. 14, Harper & Row Publishers, Inc., Philadelphia, 1992.
14. D. J. Finney, *Probit Analysis*, Cambridge University Press, Third Edition 1971.
15. S. A. Boppart, W. P. Roach, and D. X. Hammer, "Ocular and related media impurity-dependent optical breakdown thresholds for various laser pulse durations," *Bulletin of the American Physical Society*, Vol. 38, p. 318, 1993.
16. F. Docchio, C. A. Sacchi, and J. Marshall, "Experimental investigation of optical breakdown thresholds in ocular media under single pulse irradiation with different pulse durations," *Lasers in Ophthalmology*, Vol. 1, No. 2, p. 83, 1986.
17. B. Zysset, J. G. Fujimoto, and T. F. Deutsch, "Time-resolved measurements of picosecond optical breakdown," *Applied Physics B*, Vol. 48, p. 139, 1989.
18. W. L. Smith, P. Liu, and N. Bloembergen, "Superbroadening in H₂O and D₂O by self-focused picosecond pulses from a YAlG:Nd laser," *Physical Review A*, Vol. 15, No. 6, p. 2396, 1977.
19. R. R. Alfano, and P. P. Ho, "Self-, Cross-, and Induced Phase Modulations of Ultrashort Laser Pulse Propagation," *Journal of Quantum Electronics*, Vol. 24, No. 2, p. 351, 1988.
20. J. W. Boyle, J. A. Ghormley, C. J. Hochandel, and J. F. Riley, "Production of hydrated electrons by flash photolysis of liquid water with light in the first continuum," *Journal of Physical Chemistry*, Vol. 73, p. 2886, 1969.
21. D. Grand, A. Bernas, and E. Amouyal, "Photoionization of aqueous indole; conduction band edge and energy gap in liquid water," *Journal of Chemical Physics*, Vol. 44, p. 77, 1979.
22. F. Williams, S. P. Yarma, and S. Hillenius, "Liquid water as a lone-pair amorphous semiconductor," *Journal of Chemical Physics*, Vol. 64, p. 1549, 1976.